



## Exceptional activity for photocatalytic mineralization of formaldehyde over amorphous titania nanofilms



Xiao-qing Deng, Xiaobing Zhu\*, Zhi-guang Sun, Xiao-song Li, Jing-lin Liu, Chuan Shi, Ai-Min Zhu

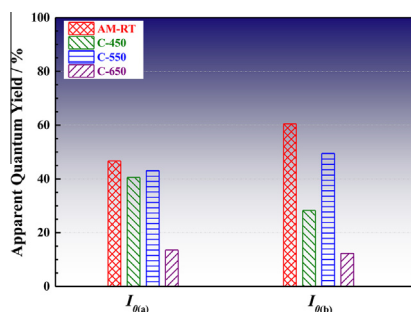
Center for Hydrogen Energy and Liquid Fuels, Laboratory of Plasma Physical Chemistry, Dalian University of Technology, Dalian 116024, China

### HIGHLIGHTS

- Amorphous titania outperformed anatase for photocatalytic formaldehyde oxidation.
- Exceptional activity is due to greatly reduced recombination and adsorption sites.
- Amorphous titania nanofilm enables photocatalysis on heat-susceptible substrates.

### GRAPHICAL ABSTRACT

Amorphous titania (AM-RT) nanofilm outperformed anatase nanofilms under UVC light (254 nm) with intensities of 1.68 ( $I_{0(a)}$ ) and 1.26 ( $I_{0(b)}$ ) mW/cm<sup>2</sup>, and achieved the highest AQY of 60.4%, for which the exceptional activity for photocatalytic mineralization of formaldehyde is attributed to greatly reduced recombination of charge carriers and abundant adsorption sites towards formaldehyde.



### ARTICLE INFO

#### Article history:

Received 13 February 2016  
Received in revised form 8 July 2016  
Accepted 3 August 2016  
Available online 3 August 2016

#### Keywords:

Photocatalytic oxidation  
Formaldehyde  
Amorphous titania  
Anatase

### ABSTRACT

As alternative photocatalysts, titania semiconductors have been extensively investigated for energy and environmental applications. However, amorphous titania is often considered not to be photoreactive catalyst. Here we demonstrate an amorphous titania thin film deposited at room temperature for a photocatalytic removal of formaldehyde from air, which features abundant hydroxyl groups and large surface area. Amorphous titania exhibited surprisingly higher apparent quantum yield of 60.4% than crystalline titania (the most active anatase). This exceptional activity is attributed to greatly reduced recombination of electron-hole pairs and abundant adsorption sites towards formaldehyde. The reduced recombination should result from rapid electron transfer along conduction band ( $>Ti^{III}OH$ ) that allocates abundant terminal hydroxyl groups, and minimized transfer length from bulk to surface in small particles. The abundant adsorption sites are related to surface hydroxyl groups and large surface area. With the exceptional activity, amorphous titania nanofilm achieved at room temperature substantially enables photocatalysis on heat-susceptible substrates, while it is nearly impossible for crystalline films calcined at high temperature.

© 2016 Elsevier B.V. All rights reserved.

## 1. Introduction

Titania semiconductor materials have emerged as the benchmark photocatalysts for energy and environmental applications due to their high activity, chemical stability, in particular resis-

\* Corresponding author.

E-mail address: [xzhu@dlut.edu.cn](mailto:xzhu@dlut.edu.cn) (X. Zhu).

tance to photo-corrosion and abundance [1–8]. Under irradiation of UV-light, the photonic excitation could generate an electron-hole pair, which gives rise to photocatalysis and super-hydrophilicity [9–14], when titania absorbs a photon of energy equal to or higher than bandgap energy. In principle, the electron-hole pair can donate the electron to an electron acceptor and oxidize a donor species by the valence band hole [14–17]. Hence, as driven by the emerging control of indoor air contaminants photocatalytic oxidation reactions can be well suited to remove volatile organic compounds (VOCs) from air [3,18].

Apparent quantum efficiency (AQY) of photocatalysts is dominated by two critical processes, which are the competition between charge carrier recombination and trapping, and the competition between trapped carrier recombination and interfacial charge transfer. The recombination of photogenerated electron-hole pairs inevitably occurs during photocatalytic reactions, causes the release of heat or light and is detrimental for quantum efficiency and photocatalytic activity [17]. In order to restrain the recombination, various investigations on doped photocatalysts as well as tailoring catalyst particle size or shape have been conducted [19–22]. The charge carriers in the trapping states are localized to particular sites in bulk phase and on surface. Charge carrier trapping would prolong the lifetime of electron-hole pair, and efficiently promote the photocatalytic reactions.

The interfacial electron-transfer rate constants and the lifetimes of charge carriers are associated with crystal defect structures and surface morphologies. Surface and bulk irregularities naturally occur during preparation processes of photocatalysts [17]. Crystalline titania materials exist in anatase, rutile and brookite, of which photocatalytic activity depends on crystallographic structure, surface area, particle size, surface hydroxyl groups, etc. In general, it can be prepared through various approaches such as sol-gel, liquid phase deposition, physical vapor deposition, chemical vapor deposition [23–26]. Consequently, correlations between photocatalytic activity (quantum efficiency) and structure emphasize the importance of an increase in either the lifetime of charge carrier or the interfacial electron-transfer rate constant [3].

Moreover, due to large intrinsic bandgap ( $E_{bg} = 3.2$  eV,  $\lambda \leq 390$  nm), titania is restricted to be activated by UV light. To more efficiently utilize the solar light ( $\lambda_{max} = 500$  nm), extensive attempts were carried out to extend the photoresponse of titania into the visible light region. State of the art photocatalysts (second generation) such as nanocomposites [27–31], Z scheme [32,33] and visible light driven photocatalysts [27,29,31–33], aim at the challenge of shifting the absorption band towards visible light but not compromising the activity. Extensive efforts have been conducted on nanocomposites/nanosheets such as anatase/brookite [28] and  $CuO_x-TiO_2$  [30] for hydrogen production, and  $Fe_2O_3-TiO_2$  [29],  $Bi_2O_{4-x}-Bi_2O_3$  [27] and carbon quantum dots hybrid with  $BiOX$  ( $X = Br, Cl, I$ ) [34,35] and  $Bi_2MO_6$  ( $M = Mo, W$ ) [36,37] for photocatalytic mineralization of organic compounds as well as plasmonic  $Au/TiO_2$  for CO oxidation [31]. Solar-driven Z-scheme photocatalysts such as Pt-SrTiO<sub>3</sub> (Cr-Ta-doped) with a redox mediator ( $I^-/IO_3^-$ ) [32], and Ir-loaded  $CoO_x/Ta_3N_5$  and Ru-loaded SrTiO<sub>3</sub> (doped with Rh) without a redox mediator [33] were demonstrated for water splitting system under visible light irradiation.

Unfortunately, amorphous titania was mostly considered as non-photoactive [9,10]. In a process of crystallization from amorphousness, it comes with surface area changes, weight loss and crystallization behavior, etc. [2]. A high surface area is usually desirable to catalytic activity, while highly amorphous mesoporous titania-silica aerogels exhibited the adverse effect of in situ adsorption of some organic substrates on the performance [4]. Amorphous hydro-oxygenated titania film prepared by plasma enhanced chemical vapor deposition exhibited photoconductivity and hydrophilicity characteristics but far below those of anatase

[25,38]. In order to enhance the photoactivity of amorphous titania, extensive efforts have been conducted on effects of film thickness [11], annealing process [10,12], photoinduced crystallization and activation [23], and the additives of metal oxides [13]. In our recent paper [39], a facile, fast and uniform deposition method to prepare amorphous titania film was developed.

Here we demonstrate an amorphous titania thin film (donated as nanofilm, around 270 nm in thickness) deposited at room temperature for the photocatalytic removal of formaldehyde from air. It features abundant hydroxyl groups and large surface area. Amorphous titania film performed surprisingly higher AQY than anatase, which is attributed to the greatly reduced recombination of electron-hole pairs and the abundant adsorption sites towards formaldehyde. The reduced recombination might result from rapid electron transfer along conduction band ( $>Ti^{III}OH$ ) in the presence of abundant terminal hydroxyl groups, and short transfer length from bulk to surface of small particles. The abundant adsorption sites are related to surface hydroxyl groups and large surface area. Chemical structural characterizations related to hydroxyl groups by X-ray photoelectron spectroscopy (XPS) and Fourier transform infrared (FTIR) spectroscopy techniques, and the measurement of adsorbed formaldehyde were conducted. Also physical structural characterizations by X-ray diffraction (XRD), atomic force microscopy (AFM), and high resolution transmission electron microscopy (HRTEM) techniques, and the measurement of BET surface area were conducted. Subsequently, the correlations between structure and activity, and the potentials of our amorphous titania nanofilm were discussed.

## 2. Material and methods

Amorphous titania thin films were deposited on quartz substrate of 19 mm (W)  $\times$  40 mm (L)  $\times$  1 mm (T) for 6 min by chemical vapor deposition (CVD) method through hydrolysis and condensation reactions of titanium precursor at room temperature under atmospheric pressure [39]. Titanium(IV) isopropoxide (TTIP, CAS # 546-68-9, 98%, J&K Scientific Ltd.) and water vapor were carried by 300 and 200 SCCM of Ar gas (99.995% purity) from two bubblers surrounded by two water baths at 50 and 20 °C, respectively. The line for TTIP delivery was heated at 60 °C to avoid its condensation. Calcined film samples of C-450, C-550 and C-650 were obtained by heating above amorphous samples in a muffle furnace at a ramp rate of 5 °C/min from room temperature to 450, 550, and 650 °C, and held for 2 h, respectively.

Surface morphology and microstructure were observed by HRTEM (Tecnai G220 S-Twin, FEI, USA) on all film samples. Also, 3D morphology images of the films were taken by AFM (solver p47 pro, NT-MDT), and the roughness was calculated by using soft NOVA 1138.2 at a window size of a  $\mu m \times a \mu m$  ( $a = 5$  or  $6$ ).

XRD patterns were operated under conditions of 40 kV and 30 mA, and recorded using  $Cu K\alpha_1$  ( $\lambda = 1.05406 \text{ \AA}$ ) radiation in step mode between 20° and 80°,  $2\theta$  at a scan rate of 2°/min (XRD-6000, Shimadzu), and between 23° and 28°,  $2\theta$  at a step size of 0.026° and 50 s duration per step (Empyrean, PANalytical). Fractional crystallinity was achieved by analysis of intensity and full width at half maximum (FWHM) of anatase (1 0 1) peak [40], with an assumption of 100% crystallinity of sample C-650 calcined at 650 °C.

The film thickness ( $d$ ) was measured by an ellipsometer (M-2000DI, J.A. Woollam). Based upon UV-vis absorption spectra measured by a UV-vis spectrophotometer (V-550, JASCO), bandgap energy ( $E_g$ ) of direct or indirect transitions is determined by Eqs. (1) and (2),

$$\alpha h\nu = B(h\nu - E_g)^p \quad (1)$$

$$\alpha = (-\lg T)/d \quad (2)$$

Download English Version:

<https://daneshyari.com/en/article/6581571>

Download Persian Version:

<https://daneshyari.com/article/6581571>

[Daneshyari.com](https://daneshyari.com)